



# Negative differential resistance induced by thermalization of two-dimensional electrons in terahertz quantum-well photodetectors

X. G. Guo,<sup>1,a)</sup> L. L. Gu,<sup>1</sup> M. Dong,<sup>1</sup> J. C. Cao,<sup>1</sup> H. C. Liu,<sup>2</sup> and F. M. Guo<sup>3</sup>

<sup>1</sup>Key Laboratory of Terahertz Solid-State Technology, Shanghai Institute of Microsystem and Information Technology, Chinese Academy of Sciences, 865 Changning Road, Shanghai 200050, China

<sup>2</sup>Key Laboratory of Artificial Structures and Quantum Control, Ministry of Education, Department of Physics, Shanghai Jiao Tong University, 800 Dongchuan Road, Shanghai 200240, China

<sup>3</sup>Key Laboratory of Polar Materials and Devices, Ministry of Education, East China Normal University, 500 Dongchuan Road, Shanghai 200241, China

(Received 10 August 2013; accepted 16 July 2013; published online 31 July 2013)

Abstract: We study the negative differential resistance (NDR) induced by thermalization of two-dimensional electrons in terahertz quantum-well photodetectors. The NDR is observed in the current-voltage (I-V) characteristics of the photodetectors under the excitation of terahertz radiation. The NDR is attributed to the thermalization of the photo-generated electrons and holes. The NDR is observed in the current-voltage (I-V) characteristics of the photodetectors under the excitation of terahertz radiation. The NDR is attributed to the thermalization of the photo-generated electrons and holes. The NDR is observed in the current-voltage (I-V) characteristics of the photodetectors under the excitation of terahertz radiation. The NDR is attributed to the thermalization of the photo-generated electrons and holes.

DOI: 10.1063/1.4808343

© 2013 AIP Publishing LLC.

## I. INTRODUCTION

Quantum-well photodetectors (QWPDs) have attracted much attention in the past few years because of their high responsivity and low noise. In a QWPD, the photo-generated electrons and holes are separated by the built-in electric field. The current-voltage (I-V) characteristics of the QWPDs show a negative differential resistance (NDR) region. The NDR is attributed to the thermalization of the photo-generated electrons and holes. The NDR is observed in the current-voltage (I-V) characteristics of the photodetectors under the excitation of terahertz radiation. The NDR is attributed to the thermalization of the photo-generated electrons and holes. The NDR is observed in the current-voltage (I-V) characteristics of the photodetectors under the excitation of terahertz radiation. The NDR is attributed to the thermalization of the photo-generated electrons and holes.

## II. THEORETICAL MODEL

The current-voltage (I-V) characteristics of the QWPDs are determined by the balance of the generation and recombination of the photo-generated electrons and holes. The current  $I$  is given by

$$I = qA \int_{E_c}^{E_v} S(E_k, J) - R(T_e, T_L) dE_k, \quad (1)$$

where  $q$  is the elementary charge,  $A$  is the area of the photodetector,  $S(E_k, J)$  is the generation rate of the photo-generated electrons and holes, and  $R(T_e, T_L)$  is the recombination rate of the photo-generated electrons and holes. The generation rate  $S(E_k, J)$  is given by

$$S(E_k, J) = \frac{J}{\hbar \omega} \frac{dN}{dE_k}, \quad (2)$$

where  $J$  is the incident power density,  $\hbar \omega$  is the photon energy, and  $dN/dE_k$  is the density of states of the photo-generated electrons and holes. The recombination rate  $R(T_e, T_L)$  is given by

$$R(T_e, T_L) = \frac{1}{\tau} \frac{N}{V}, \quad (3)$$

where  $\tau$  is the carrier lifetime,  $N$  is the total number of photo-generated electrons and holes, and  $V$  is the volume of the photodetector. The current  $I$  is given by

$$I = qA \int_{E_c}^{E_v} \frac{J}{\hbar \omega} \frac{dN}{dE_k} - \frac{1}{\tau} \frac{N}{V} dE_k. \quad (4)$$

The current  $I$  is given by

$$I = qA \int_{E_c}^{E_v} \frac{J}{\hbar \omega} \frac{dN}{dE_k} - \frac{1}{\tau} \frac{N}{V} dE_k. \quad (5)$$

The current  $I$  is given by

$$I = qA \int_{E_c}^{E_v} \frac{J}{\hbar \omega} \frac{dN}{dE_k} - \frac{1}{\tau} \frac{N}{V} dE_k. \quad (6)$$

The current  $I$  is given by

$$I = qA \int_{E_c}^{E_v} \frac{J}{\hbar \omega} \frac{dN}{dE_k} - \frac{1}{\tau} \frac{N}{V} dE_k. \quad (7)$$

The current  $I$  is given by

$$I = qA \int_{E_c}^{E_v} \frac{J}{\hbar \omega} \frac{dN}{dE_k} - \frac{1}{\tau} \frac{N}{V} dE_k. \quad (8)$$

The current  $I$  is given by

$$I = qA \int_{E_c}^{E_v} \frac{J}{\hbar \omega} \frac{dN}{dE_k} - \frac{1}{\tau} \frac{N}{V} dE_k. \quad (9)$$

$$T_{ei} = \begin{cases} \sqrt[3]{T_L^3 + aE_{ki}J}, & \text{if } T_{ei} < T \\ T_{ei}, & \text{if } T_{ei} \geq T \end{cases} \quad (1)$$

$$V = L_b F_0 + \sum_{i=1}^N (L_b + L_w) F_i, \quad (4)$$

$$T_{ei} = a, \gamma, \quad (1)$$

$$\rho_i = \rho_d + \frac{\epsilon_0 \epsilon_r}{q} (F_i - F_{i-1}), \quad (2)$$

$$p_c J_{inj}(F_0, T_L, T_e) = J_{th}(\rho_i, F_i, T_e), \quad (3)$$

$$\rho_i = \rho_d + \frac{\epsilon_0 \epsilon_r}{q} (F_i - F_{i-1}), \quad (2)$$

$$p_c J_{inj}(F_0, T_L, T_e) = J_{th}(\rho_i, F_i, T_e), \quad (3)$$

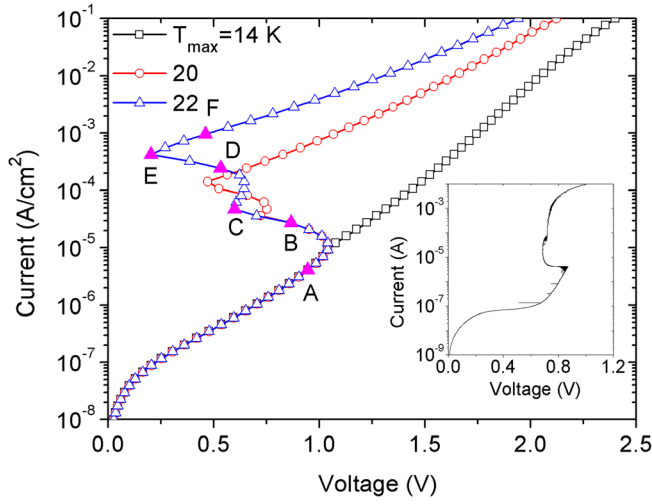
$$J_{inj} = \frac{q m^* k T_L}{2\pi^2 \hbar^3} \int_{E_c}^{\infty} T(E_z, F_0) \times \left[ \frac{1 + ((E_{Fc} - E_z)/kT_L)}{1 + ((E_{Fw} - E_z - qF_0 L_b)/kT_e)} \right] \quad (5)$$

$$T(E_z, F_0) = \begin{cases} 1, & E_z \geq E_b \\ [(-4/3qF_0)(2m^*/\hbar^2)^{1/2}(E_b - E_z)^{3/2}], & E_b - qF_0 L_b \leq E_z < E_b \\ [(-4/3qF_0)(2m^*/\hbar^2)^{1/2}(E_b - E_z)^{3/2} - (E_b - E_z - qF_0 L_b)^{3/2}], & E_z < E_b - qF_0 L_b \end{cases} \quad (6)$$

### III. NUMERICAL RESULTS AND DISCUSSIONS

Figure 8 and 14 show the numerical results for the current density  $J$  and the electron temperature  $T$  as a function of the electric field  $F_0$ . The parameters used are  $L_w = 11.9 \text{ nm}$ ,  $A = 1.0 \times 10^{-17} \text{ cm}^2$ ,  $L_b = 55.2 \text{ nm}$ ,  $A_{0.05} = 0.95 A$ ,  $\rho_d = 1.0 \times 10^{11} \text{ cm}^{-3}$ ,  $\epsilon_r = 10.88$ , and  $\gamma = 4.0$ . The current density  $J$  is calculated using the above equations. Figure 14 shows the electron temperature  $T$  as a function of  $F_0$ , which is calculated using the equation  $T_{ei} = a, \gamma, (1)$ .

Figure 10 shows the numerical results for the current density  $J$  and the electron temperature  $T$  as a function of the electric field  $F_0$ . The parameters used are  $L_w = 11.9 \text{ nm}$ ,  $A = 1.0 \times 10^{-17} \text{ cm}^2$ ,  $L_b = 55.2 \text{ nm}$ ,  $A_{0.05} = 0.95 A$ ,  $\rho_d = 1.0 \times 10^{11} \text{ cm}^{-3}$ ,  $\epsilon_r = 10.88$ , and  $\gamma = 4.0$ . The current density  $J$  is calculated using the above equations. Figure 10 shows the electron temperature  $T$  as a function of  $F_0$ , which is calculated using the equation  $T_{ei} = a, \gamma, (1)$ .



1.  $a = 1.0 \times 10^{10}$ ,  $\gamma = 4.0$ ,  $T = 14, 20, 22$  K

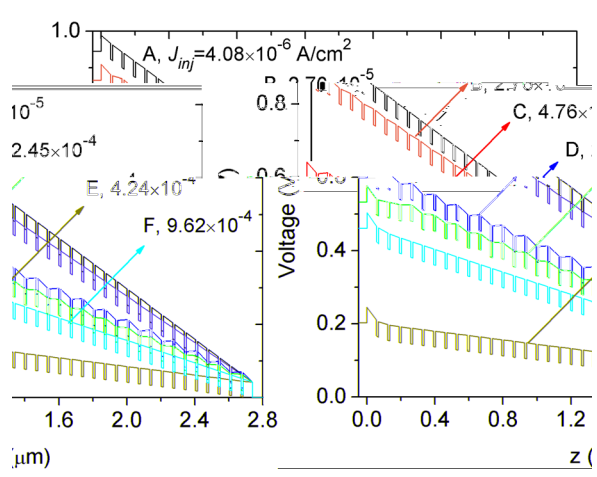
(1)

2

A,  $J_{inj} = 2.76 \times 10^{-5}$  A/cm<sup>2</sup>

1.

(t A), t



2. A,  $J_{inj} = 4.08 \times 10^{-6}$  A/cm<sup>2</sup>

1 wt  $T = 22$  K

(1), t

$T_e$

A

w

y

2

ty

ff

2

w

$J_{inj} = 2.76 \times 10^{-5}$  A/cm<sup>2</sup>

$J_{inj}$

w

ty

w

ty

et al.<sup>16</sup> At

$T_e$

$T_e$

$T_e$

A

w

2

ty

A

w

ty

2

ty

A

w

ty

2

ty

$T_e$

$T_e$

ty

2

ty

(t )

$\rho_T = \sum_{i=1}^N (\rho_i - \rho_d) / N \rho_d$

3. At

$J_{inj} > 3.0 \times 10^{-7}$  A/cm<sup>2</sup>

3

A

w

ty

2

ty

(t )

A

w

ty

2

ty

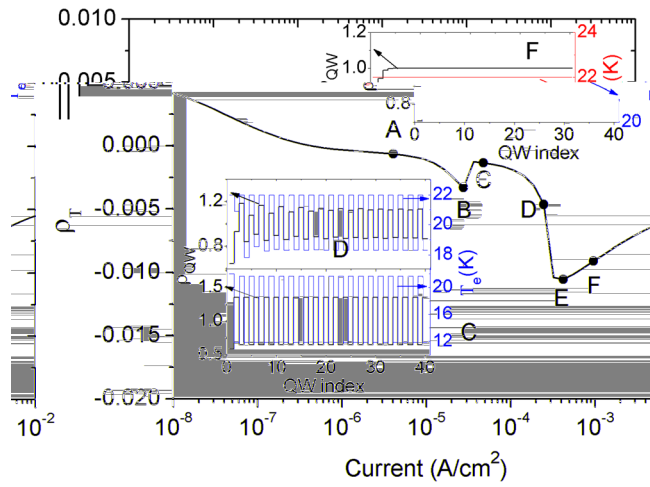
$T_e$

$T_e$

ty

2

ty



**IV. CONCLUSIONS**

**ACKNOWLEDGMENTS**

863 (2011AA010205),  
 61176086, 61131006, 60721004),  
 (2011 150021),  
 (2011 02707),  
 (2011 932903),  
 1123-1),  
 (2011 925603)  
 (91221201  
 61234005).

1. *Quantum Well Infrared Photodetectors: Physics and Applications* (2007).  
 2. *J. Appl. Phys.*, **92**, 202110 (2008).  
 3. *J. Appl. Phys.*, **110**, 013714 (2011).  
 4. *J. Appl. Phys.*, **45**, 1121 (2001).  
 5. *J. Appl. Phys.*, **19**, 219 (2004).  
 6. *J. Appl. Phys.*, **111**, 034504 (2012).  
 7. *J. Appl. Phys.*, **78**, 2902 (2001).  
 8. *J. Appl. Phys.*, **84**, 4068 (2004).  
 9. *J. Appl. Phys.*, **17**, 18 (2002).  
 10. *J. Appl. Phys.*, **79**, 446 (1996).  
 11. *J. Appl. Phys.*, **61**, 468 (1992).  
 12. *J. Appl. Phys.*, **60**, 1507 (1992).  
 13. *J. Appl. Phys.*, **74**, 1 (1993).  
 14. *J. Appl. Phys.*, **86**, 231103 (2005).  
 15. *J. Appl. Phys.*, **94**, 201101 (2009).  
 16. *J. Appl. Phys.*, **61**, 2742 (2000).